

Demonstration of all-optical phase noise suppression scheme using optical nonlinearity and conversion/dispersion delay

Mohammad Reza Chitgarha,^{1,*} Salman Khaleghi,¹ Morteza Ziyadi,¹ Amirhossein Mohajerin-Ariaei,¹ Ahmed Almaman,¹ Wajih Daab,¹ Devora Rogawski,¹ Moshe Tur,² Joseph D. Touch,³ Carsten Langrock,⁴ Martin M. Fejer,⁴ and Alan E. Willner¹

¹Department of Electrical Engineering, University of Southern California, Los Angeles, California 90089, USA

²School of Electrical Engineering, Tel Aviv University, Ramat Aviv 69978, Israel

³Information Sciences Institute, University of Southern California, 4676 Admiralty Way, Marina del Rey, California 90292, USA

⁴Edward L. Ginzton Laboratory, Stanford University, Stanford, California 94305, USA

*Corresponding author: chitgarh@usc.edu

Received January 2, 2014; revised March 21, 2014; accepted April 11, 2014;
posted April 14, 2014 (Doc. ID 203115); published May 9, 2014

We propose and demonstrate an all-optical phase noise reduction scheme that uses optical nonlinear mixing and tunable optical delays to suppress the low-speed phase noise induced by laser linewidth. By utilizing the phase conjugate copy of the original signal and two narrow-linewidth optical pumps, the phase noise induced by laser linewidth can be reduced by a factor of ~ 5 for a laser with 500-MHz phase noise bandwidth. The error-vector-magnitude can be improved from $\sim 30\%$ to $\sim 14\%$ for the same laser linewidth for 40-Gbit/s quadrature phase shift keying signal. © 2014 Optical Society of America

OCIS codes: (060.2360) Fiber optics links and subsystems; (060.4370) Nonlinear optics, fibers; (190.4223) Nonlinear wave mixing.

<http://dx.doi.org/10.1364/OL.39.002928>

Over the last several years, coherent optical communication systems have emerged as a compelling approach for enhanced data transmission performance [1]. There has been significant interest in higher-order modulation formats for optical communication systems due to the higher spectral efficiency in terms of bit/s/Hz. Specifically, quadrature phase shift keying (QPSK) is an example of 4-ary phase encoding, whereas 16 quadrature amplitude modulation is an example of 16-ary amplitude/phase encoding. In particular, QPSK has become extremely popular for currently deployed 25-Gbaud, pol-muxed 100-Gbit/s systems [1,2].

A critical limitation of phase-sensitive coherent receivers is the phase noise that exists on the recovered data signal [2]. Important sources of phase noise at the coherent receiver are the laser linewidth of the transmitter laser and of the receiver local oscillator [3–5]; note that additional sources can include nonlinear phase noise created by amplified spontaneous emission interacting with the nonlinear Kerr effect [6–8].

The traditional method to mitigate the effect of laser linewidth is to use an optical or electrical phase-locked loop (PLL) that synchronizes the frequency and phase of the local oscillator (LO) with that of the transmitter laser. The PLLs are very sensitive to the propagation delay inside their feedback loop, which can limit this method for the laser with higher linewidth [9].

Advances in high-speed very large-scale integration enable high-speed and efficient signal processing algorithms to help recover the carrier phase and partially mitigate the laser-linewidth-induced phase noise. Compared to a PLL-based receiver, these algorithms can be more tolerant to the laser phase noise since they use digital compensation techniques [9–11].

A desirable goal might be to reduce the effect of linewidth-based phase noise in coherent receivers through high-data-rate optical approaches, which might produce higher speed and wider dynamic range performance. Using the optical method, the stringent requirement on laser linewidth may be significantly lower than for other phase-recovery approaches.

In this Letter, we propose and demonstrate an all-optical scheme of phase noise reduction using optical nonlinear mixing and tunable optical delays. Utilizing the phase conjugate copy of the original signal and two narrow-linewidth optical pumps, we can reduce the phase noise induced by laser linewidth by a factor of ~ 5 for a laser with 500-MHz laser linewidth. The error-vector-magnitude (EVM) of the signal can be improved from 30% to 14% for the same laser linewidth for 40 Gbit/s QPSK signals.

The conceptual block diagram of the proposed phase noise reduction scheme is shown in Fig. 1. First, a nonlinear wave mixer generates a phase conjugate copy of the input signal by means of an injected CW laser pump. Subsequently, a liquid crystal on silicon (LCoS) programmable filter is used to filter out the CW pump and adjust the amplitudes and phases. Next, a dispersive element induces a relative delay between each signal and its corresponding conjugate copy. Finally, another nonlinear element is utilized to mix the signal, its phase conjugate copy, and another injected signal to generate the output signal [12,13].

In our proposed scheme, periodically poled lithium niobate (PPLN) waveguides are used for mixing processes in the first and second nonlinear stages. A conversion-dispersion-based delay is realized in a spool of dispersion compensating fiber (DCF) to induce a relative delay between the original signal and its replica [14].

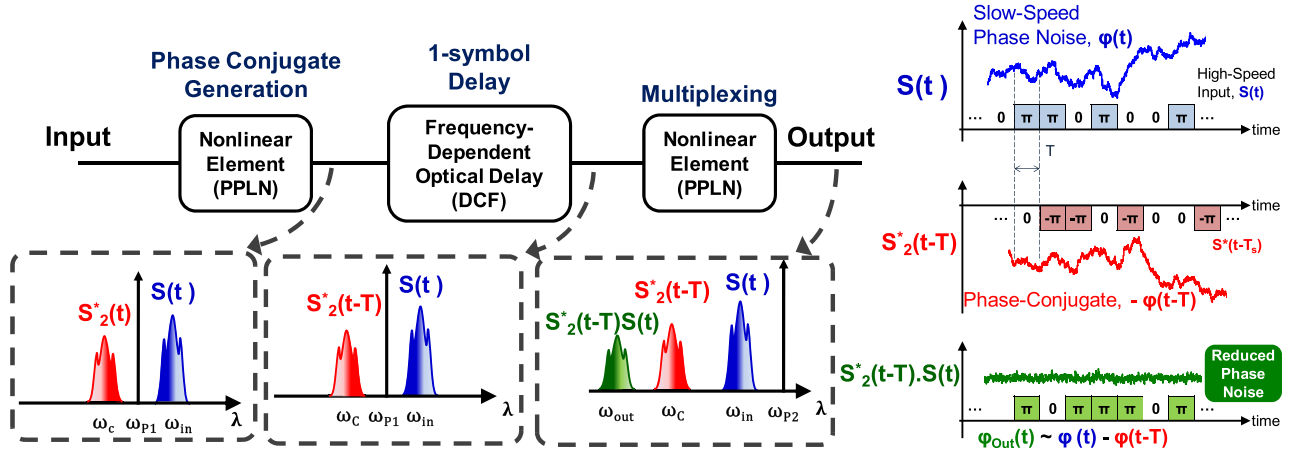


Fig. 1. Conceptual block diagram of a phase noise suppression scheme. First, a nonlinear wave mixer generates a phase conjugate copy of the input signal by using an injected CW laser pump. Next, a dispersive element induces a relative delay between the signal and its conjugate copy. Finally, another nonlinear element is utilized to mix the signal, its phase conjugate copy, and another injected signal to generate the output signal with lower phase noise.

In the first PPLN waveguide, the CW pump laser with electric field $P_1(t)$, located at quasi-phase-matching (QPM) wavelength ω_{P1} , is mixed with itself through second-harmonic generation (SHG), and they create the mixing term $P_1^2(t)$ at $2\omega_{P1}$. The SHG term then mixes with the input signals at frequencies ω_{in} through the difference-frequency-generation (DFG) nonlinear process to create phase conjugate replica at $2\omega_{P1} - \omega_{Sin}$. Given that the electric field of the input signal is $S_{in}(t)$, the electric field of the generated signal is proportional to $P_1^2(t) \times S_{in}^*(t)$.

The output of the first PPLN waveguide is sent into an amplitude- and phase-programmable filter (based on LCoS technology) followed by a frequency-dependent optical delay element (i.e., a DCF spool), in which the input signal and the corresponding phase conjugate copy are filtered, and a relative delay (T) between each signal and its corresponding conjugate copy is induced.

In the next stage, the signal $S_{in}(t)$ at ω_{in} and the delayed replica, which are located symmetrically around ω_{P1} , are mixed through a sum-frequency-generation process in the second PPLN waveguide with the same QPM wavelength. Another CW pump at ω_{P2} with electric field $S_{P2}(t)$ is also injected to the second PPLN waveguide for the DFG nonlinear process to convert the mixing product to frequency $\omega_{out} \triangleq 2\omega_{P1} - \omega_{P2}$. Hence, the electric field of the generated signal at ω_{out} can be expressed as

$$S_{out}(t) \propto P_1^2(t-T) \times S_{in}(t) \times S_{in}^*(t-T) \times P_2^*(t). \quad (1)$$

According to Eq. (1), the phase of the output signal can be obtained by using the input signal phase and the pumps' phases:

$$\Phi_{out}(t) \triangleq 2\Phi_{P1}(t-T) - \Phi_{P2}(t) + \Phi_{in}(t) - \Phi_{in}(t-T), \quad (2)$$

in which Φ_{P1} , Φ_{P2} , and Φ_{in} are the phases of P_1 , P_2 , and S_{in} , respectively. Assuming that the phase noises of the first and second pumps are negligible, we can simplify Eq. (2):

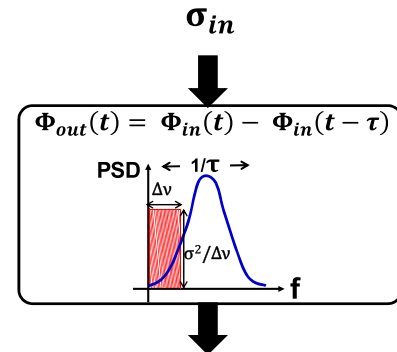
$$\Phi_{out}(t) \cong \Phi_{in}(t) - \Phi_{in}(t-T). \quad (3)$$

If the time delay between the signal and its conjugate copy is set to one symbol period and the original signal has low-speed phase noise, this phase noise can be cancelled.

Figure 2 shows how this phase noise suppression system filters out the noise part of the input phase while maintaining the data by changing only its encoding. The phase of the original signal consists of both data and the phase noise ($\varphi_{in}(t) = \varphi_{Data}(t) + \varphi_{Noise}(t)$). Therefore,

$$\begin{aligned} \varphi_{out}(t) &= (\varphi_{Data}(t) - \varphi_{Data}(t-T)) \\ &+ (\varphi_{Noise}(t) - \varphi_{Noise}(t-T)), \end{aligned} \quad (4)$$

the first row is an encoding version of the original data, which is similar to the differential phase shift keying modulation format. The second row can be viewed as a differentiator on the phase domain, which is able to filter out the low-frequency component of the phase noise (e.g., laser phase noise). By performing a Fourier transform of the noise part of Eq. (4), the following equation in frequency domain can be obtained:



$$\sigma_{out} = \sqrt{2(1 - \text{sinc}(2\Delta\nu T))} \times \sigma_{in}$$

Fig. 2. Implementing a linear differentiator in the phase domain to reduce low-speed phase noise.

$$\Phi_{\text{Noise-out}}(\omega) = 2je^{-j\omega T/2} \sin(\omega T/2) \times \Phi_{\text{Noise}}(\omega). \quad (5)$$

Assuming a white noise for the input phase with bandwidth $\Delta\nu$ and standard deviation σ_{in} , the standard deviation of the output phase noise can be expressed as

$$\sigma_{\text{out}} = \sqrt{2(1 - \text{sinc}(2\Delta\nu T))} \times \sigma_{\text{in}}. \quad (6)$$

If $\Delta\nu \ll 1/T$, then the output phase noise is significantly lower than the input phase noise, according to the equation above.

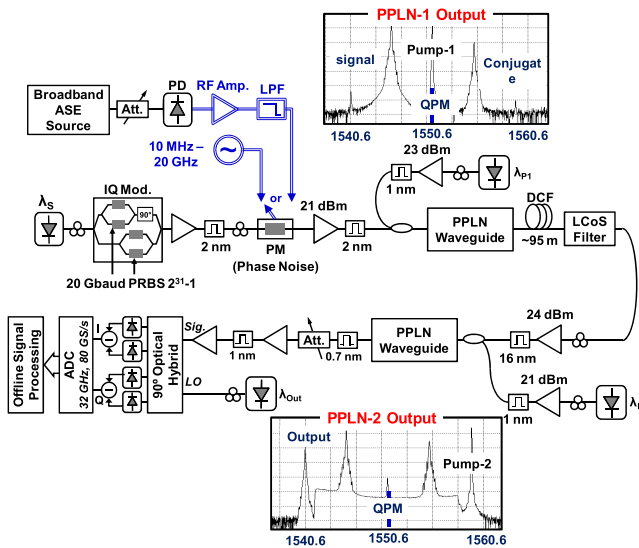
The experimental setup for the phase noise reduction scheme is depicted in Fig. 3. A nested Mach-Zehnder modulator is used to generate the 20-Gbaud binary-phase-shift-keying (BPSK) and QPSK data (PRBS $2^{31} - 1$). The resulting signal is amplified in an erbium-doped fiber amplifier (EDFA) and sent to a phase modulator that can be modulated with white noise or a sinusoidal clock. This extra stage in the transmitter is intended for inducing phase noise with different power spectral density profiles and variable standard deviations. The signal is then amplified and coupled with an amplified ~ 1550.6 nm CW pump and sent to a PPLN waveguide in order to produce the phase conjugate copy of the signal. The signal, along with its conjugate, is then sent to a ~ 50 m DCF and a spatial light modulator phase and amplitude programmable filter based on LCoS technology for adjusting the amplitudes, phases, and introducing one symbol time relative delay between the signal and its conjugate. The signal and the conjugate copy are then filtered and amplified and coupled with another amplified 1560-nm CW laser and sent to the second PPLN in order to perform mixing between the signal and the conjugate copy. The QPM wavelength of the PPLN waveguide is temperature-tuned to the QPM of the first PPLN. The mixed signal is detected coherently to EVM and phase noise. In this figure, the spectra of the first and second PPLN waveguide are also depicted. As can be seen, the wavelength separation of the signal and

its copy specifies the delay between them. In this experiment, the delay is tuned to a 50-ps delay (i.e., one symbol), and can be tuned for different baud rate [13].

In order to obtain the transfer function of the phase noise suppression scheme, a waveform generator is used to apply sinusoidal waveforms with frequencies of 250 MHz to 5 GHz on the phase of the original signal utilizing a phase modulator. Figure 4(a) shows both the theoretical curve based on Eq. (5) and the experimental data points for the ratio of the input phase noise standard deviation to the output phase noise standard deviation when the original signal is 20-Gbit/s BPSK data. While the experimental results are matched to the theory for the higher frequencies ($\nu > 750$ MHz), the data points deviate from the theoretical curve for the lower frequencies, which we believe this is the effect of other phase noise sources that dominate for lower frequencies. In Fig. 4(b), different laser linewidths between 10 kHz and 1 MHz are used for the input signal and the equivalent output linewidth is depicted. As can be seen, due to a significant reduction in linewidth of range 10 KHz to 1 MHz, the output linewidth stays ~ 60 KHz.

The performance of the system is assessed by implementing the proposed scheme on 20-Gbaud BPSK and QPSK signals that have been degraded by inducing a white phase noise at a different powers and bandwidths. Figure 5(a) shows the performance for different amounts of phase noise—all at 750 MHz bandwidth on a BPSK signal. The output of the phase noise suppression system indicates very little phase noise even in the case of high input phase noise due to the large reduction factor at the phase noise with 750-MHz bandwidth. Figure 5(b) shows the performance of the phase noise reduction scheme on a QPSK signal for a white phase noise with 100, 1000, and 3300 MHz spectral density bandwidth. The constellation points are significantly squeezed especially for the lower bandwidth.

Figure 6 shows the reduction factor for three levels of induced white phase noise ($\sigma_{\text{in}} \approx 10^\circ, 20^\circ$ and 30°) when the bandwidth of the noise source is tuned from 100 MHz to 5 GHz. The phase noise suppression scheme reduces the phase noise by filtering out the low-speed component



PM: Phase Modulator
 MZM: Mach-Zehnder Modulator
 DCF: Dispersion Compensating Fiber
 PC: Polarization Controller
 DLI: Delay Line Interferometer
 BPF: Bandpass Filter

Fig. 3. Experimental setup for the proposed phase noise suppression scheme.

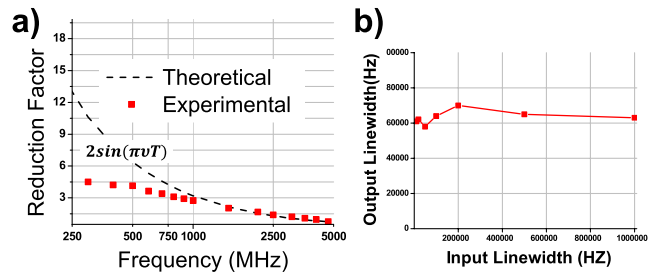


Fig. 4. (a) Ratio of input phase noise standard deviation to output phase noise standard deviation for 20-Gbit/s BPSK data. Both experimental measurement points and the theoretical curves are shown. As can be seen, the experimental results are almost aligned on the theoretical curve at higher frequencies, whereas for lower frequencies they diverge. At lower frequencies, most of the induced sinusoidal phase noise is cancelled and other sources of phase noise dominate. (b) The equivalent output linewidth for the proposed scheme versus input linewidth when lasers with 10 kHz to 1-MHz linewidths are used.

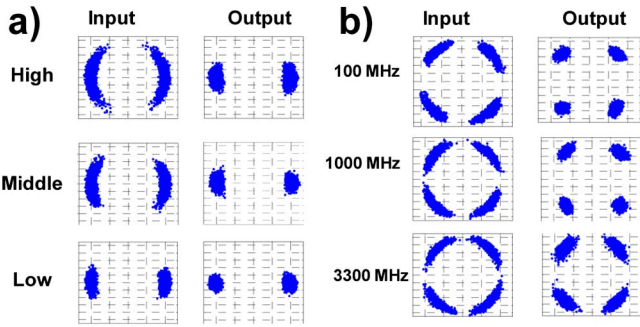


Fig. 5. (a) Phase noise reduction on 20-Gbit/s BPSK signal with constant white phase noise with different bandwidths of 750 MHz for high/middle/low phase noise standard deviations and (b) phase noise reduction on 40-Gbit/s QPSK signal with different white phase noises with bandwidths of 100 MHz/1 GHz/3.3 GHz and constant input phase noise standard deviation.

of the phase. As Fig. 6 shows, the reduction factor 0 at lower bandwidths is much higher than at higher bandwidths. Additionally, the suppression of the phase noise is higher when the higher phase noise is induced on the original signal. Figure 6 shows that this reduction factor can be as high as 3.3 for the higher phase noise at 100-MHz bandwidth, whereas the system gives very low indication of reduction of the phase noise at ~ 5 - GHz bandwidth of phase noise. Moreover, at the 750-MHz bandwidth of phase noise, the highest level of the phase noise can be decreased by a factor of ~ 2.9 , whereas the lowest level of the phase noise indicates a reduction by a factor of ~ 1.5 .

Figure 7 shows the performance of the proposed scheme by comparing the EVMs of the 40-Gbit/s QPSK signal before and after the proposed scheme. In this figure, the EVM versus frequency is depicted for the same levels of induced phase noise (i.e., $\sigma_{in} \approx 10^\circ$, 20° and 30°) for both input and output signals. In this case, the phase modulator is derived by a white noise source to illustrate the EVM improvements at different phase noise bandwidths. The EVM of the input signal is improved from 30% to 15% at the phase noise with 100-MHz bandwidth; however, this improvement is not significant for 5-GHz phase noise bandwidth (from 36% to 30%). Similar to Fig. 6, the higher phase noise experiences greater improvement in EVM. For the highest phase noise case

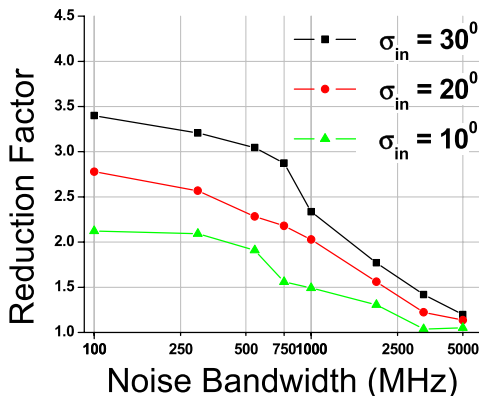


Fig. 6. Phase noise reduction factor for 40-Gbit/s QPSK signal with three levels of induced white phase noise with different bandwidths. For higher phase noise, the reduction factor is higher. On the other hand, the phase noise reduction scheme performs significantly better in lower frequencies.

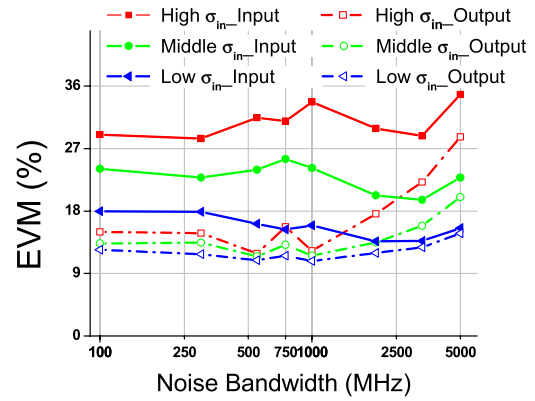


Fig. 7. EVM improvement for 40-Gbit/s QPSK signal with three levels of induced white phase noise ($\sigma_{in} \approx 10^\circ$, 20° and 30°) with different bandwidths. As can be seen, for higher phase noise, the EVM improvement is higher. On the other hand, the phase noise reduction scheme performance is better in lower frequencies.

at the bandwidth of 750 MHz, the proposed system improves the EVM from $\sim 30\%$ to $\sim 14\%$, and the lowest phase noise EVM improvement in the phase noise suppression scheme is only from $\sim 14\%$ to $\sim 10\%$. The results in Fig. 7 indicate the significant impact of the proposed phase noise suppression system on the quality of the QPSK signal.

This work was made possible by support from NSF, CIAN, DARPA, and Cisco Systems.

References

- P. J. Winzer, *IEEE Commun. Mag.* **48**(7), 26 (2010).
- E. Ip, A. P. T. Lau, D. J. F. Barros, and J. M. Kahn, *Opt. Express* **16**, 753 (2008).
- G. Colavolpe, T. Foggi, E. Forestieri, and M. Secondini, *J. Lightwave Technol.* **29**, 2790 (2011).
- C. Henry, *IEEE J. Quantum Electron.* **18**, 259 (1982).
- D. Huang, T.-H. Cheng, and C. Yu, *IEEE Photon. Technol. Lett.* **25**, 1731 (2013).
- R. Slavík, F. Parmigiani, J. Kakande, C. Lundström, M. Sjödin, P. A. Andrekson, R. Weerasuriya, S. Sygletos, A. D. Ellis, L. Grüner-Nielsen, D. Jakobsen, S. Herström, R. Phelan, J. O’Gorman, A. Bogris, D. Syvridis, S. Dasgupta, P. Petropoulos, and D. J. Richardson, *Nat. Photonics* **4**, 690 (2010).
- K. Croussore, C. Kim, and G. Li, *Opt. Lett.* **29**, 2357 (2004).
- T. Umeki, M. Asobe, H. Takara, Y. Miyamoto, and H. Takenouchi, *Opt. Express* **21**, 12077 (2013).
- E. Ip and J. M. Kahn, *J. Lightwave Technol.* **25**, 2675 (2007).
- A. Silva, M. Drummond, and R. Ribeiro, in *15th International Conference on Transparent Optical Networks (ICTON)* (2013), pp. 1–4.
- X. Shao, P.-Y. Kam, and Ch. Yu, *Opt. Express* **19**, 22600 (2011).
- M. R. Chitgarha, S. Khaleghi, Z. Bakhtiari, M. Ziyadi, O. Gerstel, L. Paraschis, C. Langrock, M. M. Fejer, and A. E. Willner, *Opt. Lett.* **38**, 3350 (2013).
- M. R. Chitgarha, S. Khaleghi, M. Ziyadi, W. Daab, A. Mohajerin-Ariaei, D. Rogawski, J. D. Touch, M. Tur, C. Langrock, M. M. Fejer, and A. E. Willner, in *Optical Fiber Communication Conference (OFC)* (Optical Society of America, 2013), paper OTh3B.
- S. Khaleghi, O. F. Yilmaz, M. R. Chitgarha, M. Tur, N. Ahmed, S. Nuccio, I. Fazel, X. Wu, M. W. Haney, C. Langrock, M. M. Fejer, and A. E. Willner, *IEEE Photon. J.* **4**, 1220 (2012).